

Kinematics of the Orion Trapezium based on Diffracto–Astrometry and Historical Data

J. Olivares¹, L.J. Sánchez¹, A. Ruelas-Mayorga¹, C. Allen¹, R. Costero¹, and A. Poveda¹

ABSTRACT

Using the novel Diffracto–Astrometry technique we analyze 44 Hubble Space Telescope Wide Field Planetary Camera 2 images of the Orion Trapezium (OT) taken over a span of 12 years (1995–2007). We measure the relative positions of the six brighter OT components (A to F), and supplement these results with measurements of the relative separations and position angles taken from the literature, thus extending our analysis time base to ~ 200 years. For every pair of components we find the relative rate of separation as well as the temporal rate of change of their position angles, which enable us to determine the relative kinematics of the system. Component E shows a velocity larger than the OT’s escape velocity, thus confirming that it is escaping from the gravitational pull of this system.

Subject headings: astrometry — stars: kinematics and dynamics — stars: individual (Theta 1 Ori) — techniques: high angular resolution

1. INTRODUCTION

With the aim of further checking the dynamical model of trapezium-type stellar systems proposed by Allen and Poveda (Poveda et al. 1967; Allen & Poveda 1974), we decided to apply the novel Diffracto-Astrometry (DA) technique, developed by Sánchez et al. (2008, 2011, 2013, in preparation), to obtain the relative motions of the most emblematic trapezium-type system: the Orion Trapezium (OT) = ADS 4186. In order to do this, we acquired precise measurements of the relative positions between the six brighter stars (components A to F) of this system.

In the past, support for this model was found by Allen et al. (1974) and Allen et al. (2004). In both these papers, studies of the relative motions of trapezium-type systems were undertaken. The work of these authors along with other contributions (e.g. Gualandris et al. (2004)) has provided enough evidence to support this model. Thus, we decided to perform a study similar to that of

Allen et al. (2004) using historical as well as modern Hubble Space Telescope data.

To obtain precise measurements of the relative positions of the OT components, we have made use of the high quality images in the HST Wide Field Planetary Camera 2 (WFPC2) public archive. Due to the fact that the OT is the trapezium-type system best studied in the astronomical literature, we also use the historical compilation of OT data contained in the Washington Double Star Catalog (WDS) maintained by Mason et al. (2001).

The majority of the images in the HST–WFPC2 archive that contain the OT was intended to study the Orion Nebula and the Orion Nebula Cluster (ONC) and, therefore, have long exposure times which result, in most cases, in saturated images of the OT components. This fact, rather than being a disadvantage, works towards our advantage, because these stellar images show diffraction spikes which are used by the DA technique to measure the position of the stars with a precision of ~ 0.1 pix (Ruelas-Mayorga et al. 2011). The diffraction spikes are produced by the supports of the secondary mirrors of both the telescope and the WFPC2. These effects, together with stellar

¹Instituto de Astronomía, Universidad Nacional Autónoma de México, Apdo. Postal 70–264, 04510, México D.F., México. e-mail: jromero@astro.unam.mx, leonardo@astro.unam.mx

image saturation, usually preclude the application of standard astrometric techniques to these images.

In Section 2 we present a brief description of the DA technique, Section 3 presents the astrometric data used to obtain the relative motions of the OT components. Section 4 contains the kinematical results and, finally, in Section 5 we present our conclusions.

2. THE DIFFRACTO-ASTROMETRY TECHNIQUE

In the past there have been attempts to perform astrometry as well as photometry on saturated sources in HST images. For example, Golimowski et al. (1995) used the diffraction spikes to do astrometry with a precision of 0.5 pixels; Gilliland¹ proposed a way to calibrate the use of the diffraction spikes to locate the photocenter of a saturated stellar image. Both Gilliland (1994) and Maíz-Apellaníz (2002) have developed somewhat different methods for obtaining photometry of saturated sources on HST images. The results appear promising. However, up to now, a definitive technique for obtaining high precision astrometric measurements has not been available.

Diffraction-Astrometry is a technique developed with the intention of obtaining high precision measurements of relative stellar positions on saturated stellar images (Sánchez et al. 2008). To establish a position for a saturated stellar image, DA utilizes in principle both the diffraction spikes and the diffraction rings on the images. So far, we have only explored the use of the diffraction spikes to determine the photocenter of saturated stars on HST-WFPC2 images of the OT. This technique recovers the positions of the photocenters taken as the intersection of a pair of lines fitted to the structure of the diffraction pattern; see Sánchez et al. (2011) and Olivares et al. (2011) for details.

The application of the DA technique to the measurement of relative stellar positions on archival HST images requires an algorithm to ensure minimum systematic errors in the results (Sánchez et al. 2008, 2011, 2013, in preparation). The measuring algorithm is designed to detect only those sections of the spikes that present a large contrast. If at

some point the faint spikes of any component are heavily interfered by the glare of a brighter component, or if their contrast is too low, the algorithm simply discards these spikes and the measurement cannot be carried out. On several images, particularly those with short exposure times in narrow-band filters, the stellar spikes are not present for every star or their contrast is too low; thus, it was not possible to measure every star on every HST image used.

2.1. Data Corrections

There exist a number of systematic errors associated with the WFPC2 measurements which have been extensively analyzed in the past. The most important are: geometric distortion (Kozhurina-Platais et al. 2003; Anderson & King 2003), the 34th row error (Anderson & King 1999), charge transfer efficiency (CTE) (Holtzman et al. 1995; Stetson 1998; Whitmore et al. 1999; Dolphin 2000), and plate scale variations (McMaster et al. 2008; Gonzaga & Biretta 2010).

The OT images used in this analysis were corrected for geometric distortion and the 34th row error using the formulae given by the listed above authors. In the case of geometric distortion, there are published transformation coefficients only for filters F300W, F555W and F814W. For those images taken with other filters, the distortion coefficients used were those pertaining to the nearest filter in wavelength, for which such coefficients exist in the literature.

It is known that CTE affects astrometry in Advanced Camera for Surveys Wide Field Channel (ACS/WFC) (Kozhurina-Platais et al. 2007). However, to our knowledge, there is no correction for CTE effects on WFPC2 astrometry (Gonzaga & Biretta 2010). In addition, according to McMaster et al. (2008, p. 103), “Images with high background signal suffer relatively little charge loss because the background signal fills the traps and prevents them from robbing the charge packets during readout.” Since the OT region is projected over the Orion Nebula, the background that these images have is relatively high ($\sim 200 e^-$ for images with exposure times $\geq 10 s$), rendering the CTE effect negligible even for the fainter E and F component spikes.

In order to account for possible changes in plate

¹Gilliland, R. L. 2007, HST Proposal 11509, Cycle 16

scale due to the use of different wavelengths, we have used all the plate scales reported in Table 5.10 of McMaster et al. (2008), and obtained interpolated values for other filters.

3. DATA

In this paper we use OT astrometric data, position angle (PA) and separation, from two different sources. One is the historical compilation of the WDS, maintained by Mason et al. (2001); the second is data obtained by us applying the DA technique to OT WFPC2 saturated images. In both these compilations, the PA values are referred to the North Celestial Pole at their corresponding epoch. Hence, the measured PAs were precessed to J2000.0 using the expression given by Argyle (2004, p. 276) for objects located far from the celestial poles, which is the case of the OT. The maximum correction applied, to the earliest epoch, amounts to $\sim 1.0^\circ$.

3.1. Astrometric Data from the Historical Compilation

Separations and position-angles between OT stellar pairs were obtained from the WDS. Data in this compilation are given with no uncertainties, so we selected only those for which we can assign realistic errors. For this reason, we only used data for those observers classified as “Best” and “Good” in Table 1 of Allen et al. (2004). As stated by these authors, the error bars in separation were assigned by C. Worley “based on a life-time of experience”. In that study, only the measures for the relative separations were used, because the historical position angles were considered less reliable.

In the present study, the uncertainties for the historical PA observations were estimated from the dispersions of different measurements by the same observer, pair of components, and epoch. These measurements were found to be considerably less reliable than those for the separations.

3.2. HST–WFPC2 Images

The HST public database (Mikulski Archive for Space Telescopes²) was meticulously inspected in order to find Orion Trapezium images with the

²<http://archive.stsci.edu/hst/>

highest astrometric quality. The selection criteria were the following: (i) We only use images taken with the WFPC2. Since the WFPC2 is fixed on the axis of the HST, the images taken with it have a very good optical quality; (ii) the OT image must be present in one of the 4 detectors, to avoid inter-chip errors due to different reference frames; (iii) the stellar components to be measured must not lie within the first ~ 50 x and y pixels; in this region the pyramid mirror makes it impossible to perform accurate astrometry; (iv) the background of the images must be $\sim 200 e^-$ in order to avoid position shifts due to CTE losses and, (v) the diffraction pattern produced by the supports of the secondary mirrors (of both telescope and camera), must be present in at least two images of the OT components.

We used 44 images that fulfilled these criteria. These images were downloaded in waived FITS (c0f.fits) format, and were already calibrated by the standard pipe-line procedure. Their characteristics are listed in Table 1.

Images are distributed in eight epochs, spanning from 1995 March 21, to 2007 November 6. 56% of the images were taken in 1995, 16% in 2007, and the rest during different years of the observing period (1995–2007). The images have a mean exposure time of ~ 120 seconds. 68% of them were taken using narrow-band (N) filters, while 28% were taken using wide-band (W) and medium-band (M) filters. 36% were taken with Detector 4, 27% with Detector 3, and the rest with Detector 1; no images taken with Detector 2 were used in this analysis. As an example, Fig. 1 shows one of the images used in this work.

3.3. Precision of Diffracto-Astrometry

Ruelas-Mayorga et al. (2011) presented an analysis of the accuracy with which the DA technique is able to recover the photocenter of a simulated Point Spread Functions (PSFs) of the WFPC2. We present here the results of a similar analysis of the DA precision on real WFPC2 images. In order to do this, we selected 25 images, from our data set, taken in one epoch only: 1995 March 21; in this way we avoid errors associated with individual motions of the stars. These images were taken with Detectors 1 and 4 (11 and 14 images, respectively) in mid and narrow band filters (3 and 22 images, respectively).

Table 1: WFPC2 Images of the Orion Trapezium.

Name	Date (UT)	Exps. Time (secs)	Filter	Detector
u2id0101t	3/21/95 5:20	180	F673N	4
u2id0104t	3/21/95 5:39	100	F631N	4
u2id0107t	3/21/95 5:49	30	F547M	4
u2id010dt	3/21/95 7:02	180	F502N	4
u2id010ft	3/21/95 7:12	60	F656N	4
u2id010it	3/21/95 7:28	180	F658N	4
u2id010jt	3/21/95 8:27	180	F673N	4
u2id010nt	3/21/95 8:52	180	F631N	4
u2id010pt	3/21/95 9:05	180	F502N	4
u2id010rt	3/21/95 10:09	180	F502N	4
u2id010tt*	3/21/95 10:18	30	F547M	4
u2id010vt	3/21/95 10:23	60	F656N	4
u2id010yt	3/21/95 10:33	180	F658N	4
u2id0110t	3/21/95 11:40	180	F658N	4
u2id0111t	3/21/95 11:49	100	F673N	1
u2id0112t	3/21/95 11:52	100	F673N	1
u2id0113t	3/21/95 11:55	100	F673N	1
u2id0114t	3/21/95 11:59	100	F631N	1
u2id0115t	3/21/95 12:02	100	F631N	1
u2id0118t	3/21/95 12:12	100	F502N	1
u2id0119t	3/21/95 12:15	100	F502N	1
u2id011at	3/21/95 12:19	30	F547M	1
u2id011et	3/21/95 13:22	60	F656N	1
u2id011gt	3/21/95 13:29	100	F658N	1
u2id011ht	3/21/95 13:32	100	F658N	1
u3j1030ar*	4/4/98 5:00	160	F656N	4
u4zj0401r	12/7/98 12:27	60	F547M	1
u4zj0402r*	12/7/98 12:31	60	F791W	1
u4zj0405r	12/7/98 12:49	500	F547M	1
u3j1050ar*	9/20/99 14:30	60	F547M	3
u6c60102r	3/12/01 22:43	30	F336W	1
u6c60108r*	3/13/01 1:56	30	F439W	1
u6eb0102m*	2/13/02 2:09	400	F502N	4
u93k3901m	4/10/05 17:10	80	F439W	3
u93k3902m*	4/10/05 17:14	10	F814W	3
u93k3904m	4/10/05 17:28	400	F336W	3
u93k3905m	4/10/05 17:38	400	F656N	3
u9w10401m	11/6/07 13:44	40	F502N	3
u9w10403m*	11/6/07 13:49	40	F547M	3
u9w10406m	11/6/07 13:56	40	F656N	3
u9w10408m	11/6/07 14:01	40	F658N	3
u9w1040am	11/6/07 14:06	40	F673N	3
u9w1040cm	11/6/07 14:13	40	F791W	3
u9w1040em	11/6/07 14:18	40	F953N	3

*Frames used as reference for each epoch listed in Tables 2 and 3.

In every one of the WFPC2 images mentioned in the previous paragraph, the stellar photocenter positions, as well as their precision, were measured as indicated in Section 2 of Ruelas-Mayorga et al. (2011). The precision of all these measurements was analyzed as a function of detector, filter, spike's effective Signal-to-Noise (eS/N) and aver-

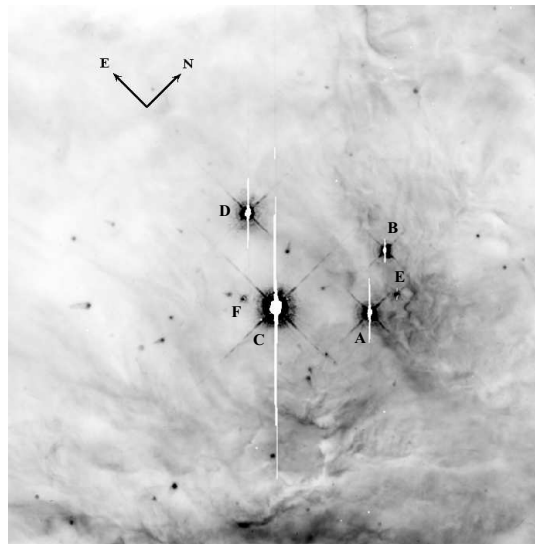


Fig. 1.— Orion Trapezium image (u2id010yt). It was taken using the WFPC2 Detector 4, in filter F658N, with 180 seconds of exposure time. The names of the six brighter components have been marked.

age effective length; the last two quantities are defined below.

To determine the eS/N of one single point in the spike, a cut – 21 pix for Detectors 2, 3 and 4 (WF) and 33 pix for Detector 1 (PC) – perpendicular to the spike at that point is performed. The point's eS/N is obtained as follows: (i) the length of the cut is divided in three equal sections; (ii) the average intensity of the two outer sections is calculated; (iii) the maximum of the central section is obtained; and (iv) the eS/N is calculated as the ratio of the maximum value calculated in (iii) to the average value derived in (ii). The spike's eS/N was computed as the average of the eS/N values of all the points along the spikes used for establishing a stellar position.

The average effective length of a spike associated with a stellar photocenter measurement is defined as the average number of points along the four spikes used to determine the photocenter position.

As an example of the precision determination we present, in Fig. 2, a plot of the distribution of uncertainties as a function of spike average length. It is clear from this figure that the value of the

precision improves, as expected, with the average length of the spikes. It seems that the precision may not be improved further than ~ 0.01 pix with this technique. However, it was found that the DA precision is, for all cases, smaller than 0.11 pix.

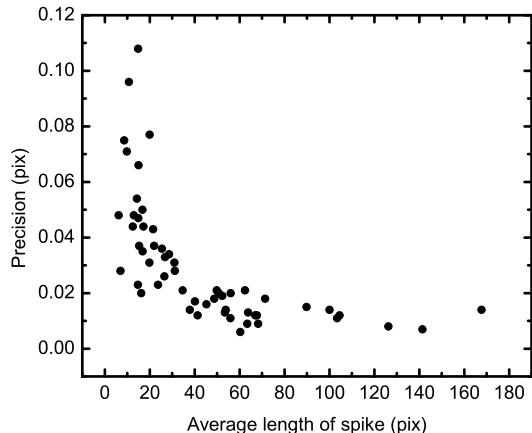


Fig. 2.— Precision of the DA technique as a function of spike average length. Solid dots represent the measurements for Detector 4 (WF).

3.4. Astrometric Data from the Diffractometric Astrometry Technique

In each of our 44 images, we measured all present OT components together with at least 9 (29 at most) unsaturated field stars. The position of the saturated stars was measured using the DA technique, while the position of the unsaturated ones was estimated using Lorentzian fitting algorithms. Positions were grouped by epoch and a reference frame was established for each one of these; we used as a reference frame the image with the largest number of measured unsaturated positions. In Table 2 we list the epochs of all the reference frames, together with their corresponding filter, detector, and plate scale. Using the *geomap* task of IRAF³ and all unsaturated positions of the epoch reference frame as pivots, we obtain a transformation between each image and its epoch reference frame. These transformations allow us

³<http://iraf.noao.edu/>

to map the positions of the OT components (A to F) on this epoch pixel-corrected reference frame. These positions are reported in Table 3.

Table 2: Plate-scales for epoch reference frames.

Epoch	Filter	Detector	Plate-Scale ^a	Matched Frames
1995.21	F547M	4	99.6583	25 ^b
1998.25	F656N	4	99.6923	1
1998.93	F791W	1	45.5733	3
1999.72	F547M	3	99.6147	1
2001.19	F439W	1	45.5468	2
2002.12	F502N	4	99.6631	1
2005.27	F814W	3	99.6529	4
2007.84	F547M	3	99.6147	7

^aPlate-scales interpolated from those reported by McMaster et al. (2008). Units are mas pixel⁻¹ (± 0.005 for the PC and ± 0.01 for the WF detectors).

^bFor this epoch, the 11 PC frames were also matched to WF4 F547M epoch reference frame.

Using the positions of the photocenters reported in Table 3, together with their corresponding plate-scales in Table 2, we were able to measure, for every pair of components, the separation (in arcseconds) and the PA (in degrees, measured by convention, from North to East).

The North direction was established using the group keyword ORIENTAT given in the header of each WFPC2 image. This keyword records the angle, in degrees, between the North and the columns of the detector; it is measured from North to East. Determination of the North direction is limited by the HST guide stars positions, the mode in which these stars were acquired by the Fine Guidance Sensors (FGS), and the transformation between FGS and WFPC2. In all of our images, the FGS’s acquisition mode was FINE; this mode renders a typical rms pointing precision better than 2 to 5 mas (Fruchter & Sosey 2009). These figures, transformed to the WFPC2, provide an absolute astrometry accuracy between 0.5 and 1 arcsec (Gonzaga & Biretta 2010).

The entire list of measurements, both from WDS and DA, can be obtained from the authors by request.

A combination of OT–astrometric data from the WDS and DA-measurements of 44 OT HST-images allows us to present in the next section the internal motions of the OT.

Table 3: WFPC2 astrometry of OT components A to F, for different epochs.

Epoch	Pixel Coordinates (x, y) ^a					
	A		B		C	
1995.21	417.12 ± 0.13	350.18 ± 0.15	370.66 ± 0.11	426.02 ± 0.31	320.88 ± 0.09	263.77 ± 0.17
1998.25*	630.03 ± 0.06	386.73 ± 0.06	583.47 ± 0.10	463.08 ± 0.10	533.58 ± 0.01	300.15 ± 0.01
1998.93	617.05 ± 0.16	499.62 ± 0.14	515.18 ± 0.10	665.80 ± 0.22	406.18 ± 0.19	311.20 ± 0.08
1999.72*	377.11 ± 0.01	321.99 ± 0.01	330.25 ± 0.03	397.85 ± 0.03	280.24 ± 0.01	235.65 ± 0.01
2001.19	327.45 ± 0.13	222.94 ± 0.01
2002.12*	422.46 ± 0.08	426.42 ± 0.08	375.82 ± 0.09	501.94 ± 0.09	326.50 ± 0.05	340.06 ± 0.05
2005.27	414.90 ± 0.11	380.65 ± 0.20	368.48 ± 0.33	456.43 ± 0.18	318.36 ± 0.09	294.16 ± 0.02
2007.84	445.50 ± 0.12	532.05 ± 0.10	399.15 ± 0.13	608.12 ± 0.08	349.30 ± 0.07	445.51 ± 0.10
	D		E		F	
1995.21	201.95 ± 0.17	327.44 ± 0.12	424.91 ± 0.12	394.80 ± 0.23	282.04 ± 0.26	240.60 ± 0.25
1998.25*	414.40 ± 0.05	364.13 ± 0.05	637.92 ± 0.07	431.70 ± 0.07
1998.93	146.00 ± 0.10	450.50 ± 0.09	634.38 ± 0.17	597.65 ± 0.20	321.04 ± 0.17	260.97 ± 0.08
1999.72*	161.34 ± 0.01	299.43 ± 0.01	385.59 ± 0.05	366.91 ± 0.05
2001.19	67.35 ± 0.06	362.21 ± 0.08	241.64 ± 0.08	171.85 ± 0.14
2002.12*	207.97 ± 0.11	403.78 ± 0.11
2005.27	199.28 ± 0.41	358.01 ± 0.24	422.69 ± 0.10	425.18 ± 0.12	278.86 ± 0.23	271.07 ± 0.04
2007.84	230.63 ± 0.16	509.41 ± 0.13	453.15 ± 0.05	576.62 ± 0.04

^a Coordinates (x and y) in the system of epoch reference frame, corrected for geometric distortions. Increasing y is to the North, and increasing x is to the West. Uncertainties are given as the standard deviation, except for those cases marked by an asterisk, in which they correspond to the DA technique precision.

4. KINEMATICS OF THE ORION TRAPEZIUM

4.1. Astrometric Results

To determine the internal kinematics of the OT components, we performed linear least-squares (LSQ) fits to the separation and the PA, both for WDS as well as DA data, as a function of time.

As examples of the relative motions of the OT components, we present Figs. 3 to 6 in which we plot the values for the separation and the PA of the component pairs AC, AE, CB and CD, as a function of time. The straight line resulted from linear LSQ-fits to the points.

Since the precision of the PA historical measurements is low, as stated in Section 3.1, and the time base of the DA measures is relatively short, the rates of change derived from the fit to the PA data are significantly less reliable than those obtained for the fits to the separation data.

Tests for membership of OT components A to E to the Trapezium were already performed by Allen et al. (2004). However, in that study it was not possible to establish the physical membership

of component F to the OT, due to the fact that component C shows widely discrepant values for its proper motion (Jeffers et al. 1963; Mason et al. 2001) and hence the proper-motion test for pair CF could not be carried out. Given the large transverse velocity of F relative to C derived from our measures for the PA and separation velocities ($11.2 \pm 0.8 \text{ km s}^{-1}$ and $2.7 \pm 0.9 \text{ km s}^{-1}$, respectively) we think it is a foreground star. It is probably related to the stellar population located in front of the ONC, as proposed by Alves & Bouy (2012). In view of this fact, we decided to disregard the kinematical information of this component.

The relative motions of components A to E of the OT are summarized in Table 4. In this Table, the first column indicates the pair of OT components, the second and third the rate of change in PA and separation, respectively. The figures in the last two columns were transformed to km s^{-1} adopting a distance to the Orion Nebula of $414 \pm 7 \text{ pc}$ (Menten et al. 2007). The precision of these relative velocity determinations was found to be $\sim 1.0 \text{ km s}^{-1}$; this value corresponds to the average of uncertainties in Table 4.

Finally, we note that the results presented in

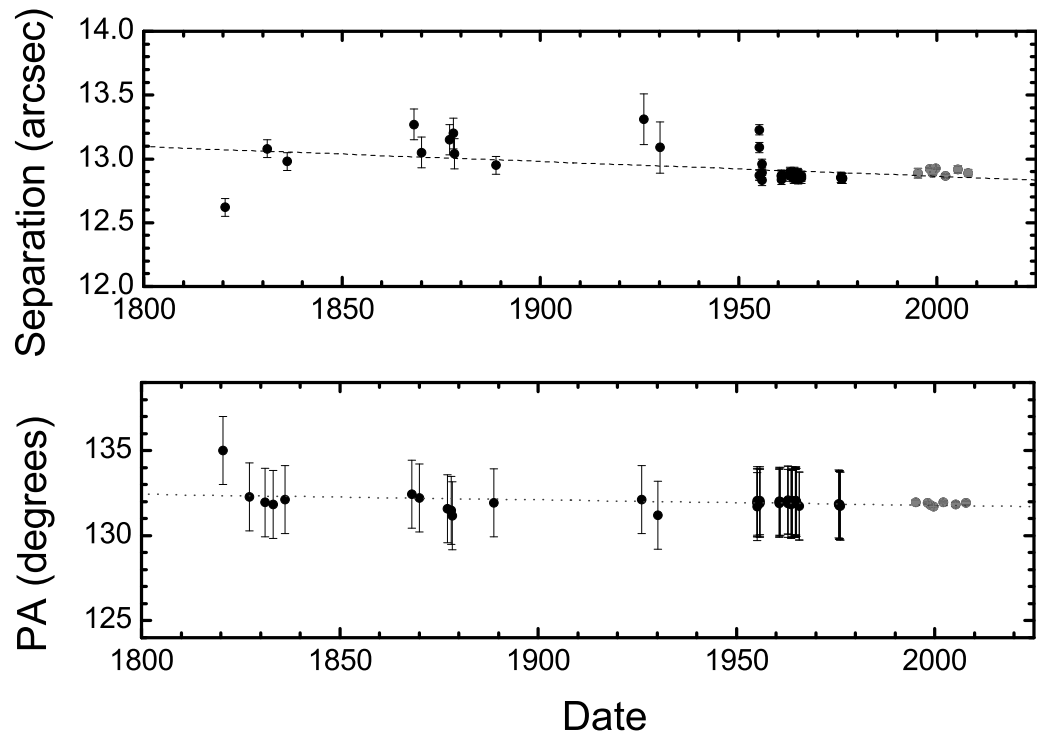


Fig. 3.— Separation and precessed PA of component C relative to A, as a function of time. Black circles correspond to WDS data with its associated error bars. Gray circles denote DA data with its associated error bars (smaller than symbol). The lines show the best LSQ-fit to the data.

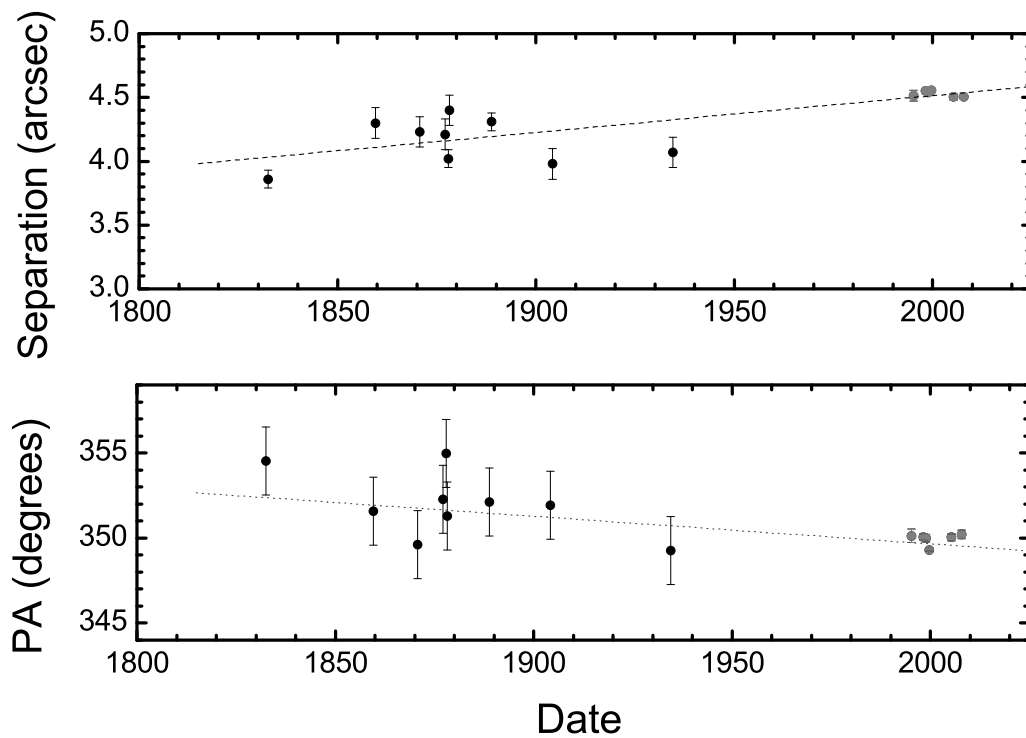


Fig. 4.— Separation and precessed PA of component E with respect to component A as a function of time. Symbols and lines as in Fig. 3. Complementing this information with radial velocity measurements from Costero et al. (2008), we confirm that component E is escaping from the Trapezium.

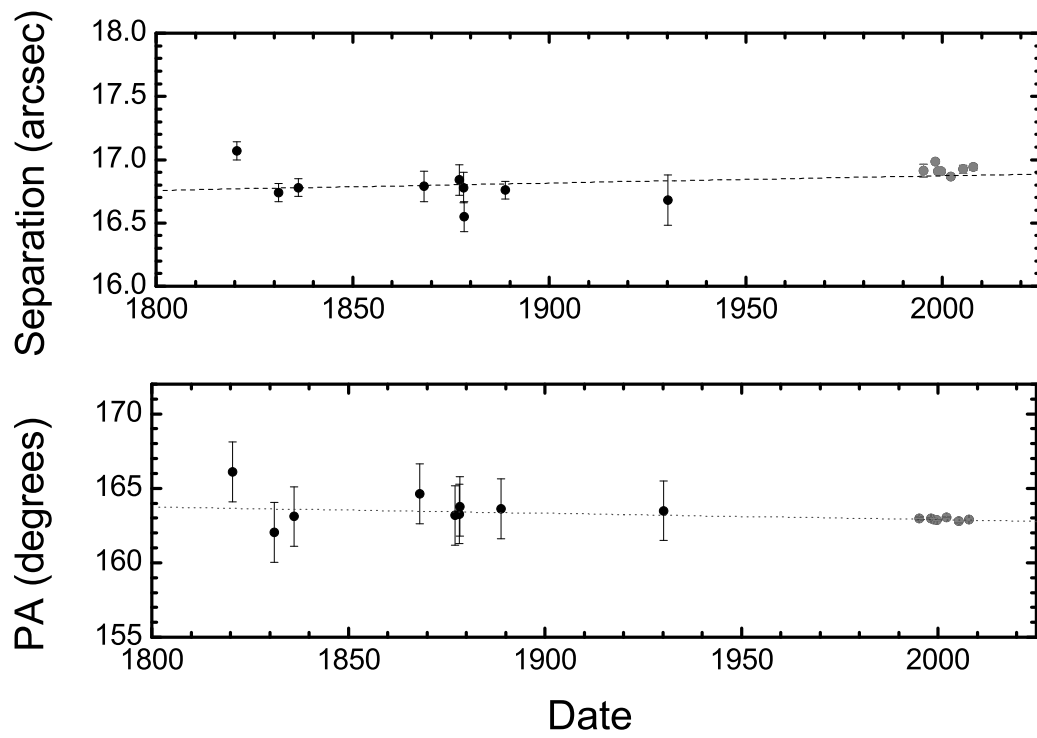


Fig. 5.— Separation and precessed PA of component B with respect to component C as a function of time. Symbols and lines as in Fig. 3.

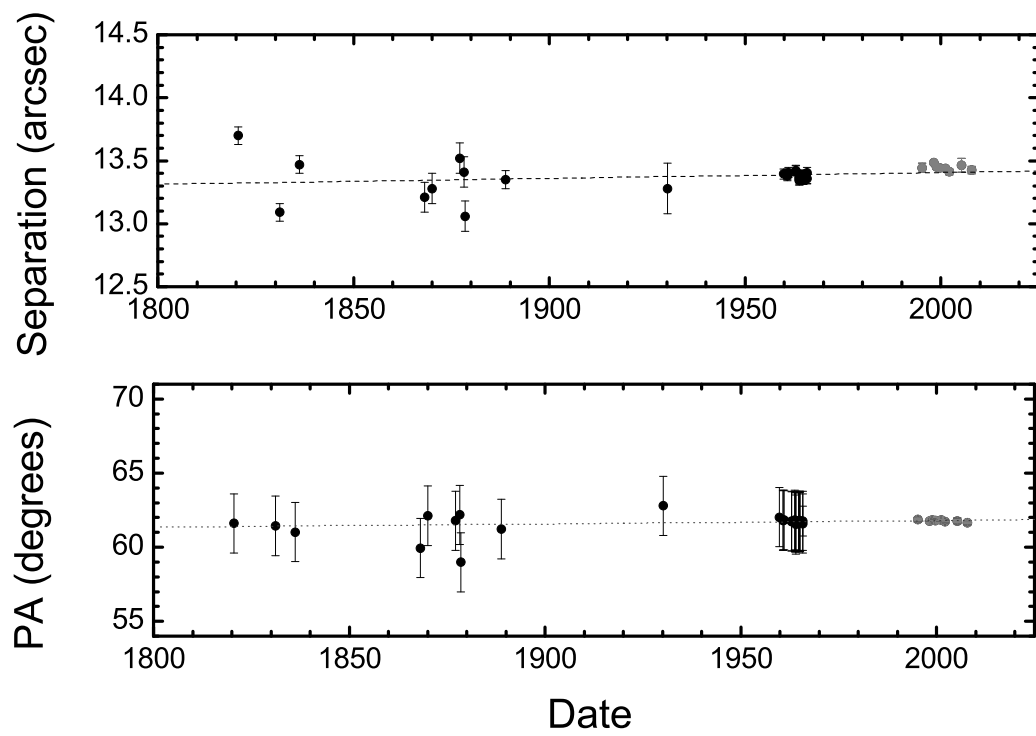


Fig. 6.— Separation and precessed PA of component D with respect to component C as a function of time. Symbols and lines as in Fig. 3.

Table 4: Temporal rate of change of PA and Separation.

Pair	PA Velocity (km s ⁻¹)	Separation Velocity (km s ⁻¹)
AB	-0.7 ± 0.8	4.1 ± 0.5
AC	-1.4 ± 0.5	-2.3 ± 0.7
AD	-1.5 ± 0.4	1.6 ± 0.4
AE	-2.9 ± 0.9	5.5 ± 1.2
BC	-3.4 ± 1.7	1.4 ± 0.9
BD	-0.5 ± 0.7	2.8 ± 0.4
BE	0.5 ± 0.8	-1.4 ± 0.9
CD	1.5 ± 0.7	0.9 ± 0.6
CE	-0.4 ± 1.0	-5.7 ± 0.8
DE	1.9 ± 1.0	5.0 ± 1.2

this section are fairly consistent with those published by Allen et al. (2004). These authors determine the magnitude of the relative motions between pairs AB, AC and AE as +0.18, -0.11, and +0.36 seconds of arc per 100 years, respectively, disregarding the changes in PA. A transformation of these motions to transverse velocities results in +3.6, -2.2, and +7.1 km s⁻¹, respectively, again using 414 ± 7 pc for the distance to the Orion Nebula (Menten et al. 2007).

4.2. Heliocentric Radial Velocities and Multiplicity

θ^1 Ori A is a spectroscopic and eclipsing binary (V1016 Ori). Its systemic radial velocity has been obtained by Vitrichenko et al. (1998) and Stickland & Lloyd (2000). Based on essentially the same previously published data and a few additional data points of their own, both groups obtain the value given in Table 5. The star is, in addition, an interferometric binary under close scrutiny (see Preibisch et al. (1999); Close et al. (2012)).

Itself a spectroscopic and eclipsing binary, the orbital parameters of θ^1 Ori B (BM Ori) have been obtained by several authors. Vitrichenko & Klochkova (2004) notice that the values of the systemic velocity published for this system differ significantly between authors and, hence, between epochs. To reconcile previous results with their own, these authors postulate a third component in a 3.57 year,

highly eccentric orbit. In Table 5 we have adopted the systemic velocity of the putative triple system, as given by Vitrichenko & Klochkova (2004). This system is part of a “mini-cluster”; see Close et al. (2012).

θ^1 Ori C, the brightest member of the Trapezium, is an interferometric binary whose primary component is probably a spectroscopic binary system (Vitrichenko 2002). Complicated by line-profile periodical variability associated with the oblique magnetic rotator character of the brightest component, no reliable systemic radial velocity is available for this binary. We have adopted 23.6 km s⁻¹, a value obtained by Kraus et al. (2009) by adjusting published radial velocity values for the primary component to that derived from the interferometric binary orbit. No error was associated to this barycentric velocity in that paper, but its value is nearly equal to the average of those obtained recently by Lehmann et al. (2010) and Vitrichenko et al. (2012) for the close binary ($P \simeq 61$ d). A conservative guess of the error associated with it is ± 2 km s⁻¹.

It is frequently assumed that θ^1 Ori D is a single star. However, since the time that its radial velocity was first measured (Plaskett & Pearce 1931), it was considered to be a spectroscopic binary. Indeed, Vitrichenko (2002b), using all available velocity data, including his own measurements on IUE spectra, derived preliminary orbital elements, with two possible solutions for the orbital period that differ from each other by a factor of two. The value for the systemic velocity of this object given in Table 5 is that for the shorter period solution, preferred by the author, but the error we associate with it is three times larger than that given in his paper, since it is representative of the difference between the systemic velocity as derived from both solutions. In addition, this star is probably a visual binary (Close et al. 2012).

The values for the systemic velocity for θ^1 Ori E and F come, respectively, from Costero et al. (2008) and Costero et al. (in preparation).

We stress the fact that the uncertainties in Table 5 are probably gross underestimates. The radial velocities quoted are also very uncertain.

As stated above, several of the OT components are multiple stars. In principle, the orbital motion of a secondary component around its primary

Table 5: Radial velocities of Trapezium stars

Name	v (km s^{-1})
θ^1 Ori A	28 ± 1
θ^1 Ori B	26 ± 1
θ^1 Ori C	23.6 ± 2.0
θ^1 Ori D	32.4 ± 3.0
θ^1 Ori E	34.3 ± 1.0
θ^1 Ori F	20 ± 4

may produce displacements of the primary that could be confused with relative motions with respect to other components of the OT. However, we note that the only component whose orbital motion could be of the order of the DA errors in the measures is component C. The maximum relative orbital displacement that component C could show (see Table 3 in Kraus et al. (2009)) is 43 mas over one orbital period. Since the mass ratio of the components is at most 0.23 (Kraus et al. 2009) the displacement due to orbital motion of component C would be at most 10 mas, smaller than our measurement errors, which are of the order of 20 mas for the relative position. All other components have either spectroscopic companions, or else very large separations with correspondingly long periods (much larger than the span of our measurements).

Particularly, in the case of component A, the system A1-A2 is probably a physical binary (Close et al. 2012). Assuming a circular orbit for the system and 0° inclination, a period of about 400 years is deduced from the change in PA of $0^\circ.92 \pm 0^\circ.07$ per year (Close et al. 2012). In this case, taking a separation of $0.20''$ and a mass ratio of 0.2 (Weigelt et al. 1999), component A1 will show an oscillation, about the barycenter, of $0.08''$ in 200 years. Such an oscillation is much smaller than the precision of the WDS data, and hence undetectable.

On the other hand, the WFPC2 measurements are essentially coeval with those of Close et al. (2012) who report a separation rate of -1.4 ± 0.22 mas yr $^{-1}$ between A1 and A2; this translates into a 0.28 mas yr $^{-1}$ movement of A1 towards the barycenter, which is an order of magnitude smaller than our reported 2.8 ± 0.6 mas yr $^{-1}$ rate of sepa-

ration between A and E.

The effect of the orbital motion of A1-A2 on the PA between A and E on the WFPC2 measurements depends on the configuration between A1, A2 and E which, during the observation period, was such that the three stars were nearly aligned; consequently, the PA yearly rate of change reported by Close et al. (2012) for A1-A2 ($0^\circ.92$ yr $^{-1}$) translates into almost $0^\circ.1$ change in PA for pair AE during the 12 years lapse of the WFPC2 measurements used. In nearly 200 years, the change in the PA of the pair of objects A1-E would oscillate, assuming a circular apparent orbit for A1-A2, with an amplitude of $0^\circ.9$. These effects are of the same order as the errors of a single WFPC2 and WDS datum, respectively, and consequently undistinguishable, as can be noted in Fig. 4.

We conclude that the orbital motions due to multiplicity of the OT members do not affect either the measurements carried out by the DA technique, or those of the WDS compilation.

4.3. Status and internal velocity dispersion of the Orion Trapezium

The most important kinematical results are as follows:

- The value we derive for the rate of change of the separation of component E relative to A, 5.5 ± 1.2 km s $^{-1}$, although smaller than that reported by Allen et al. (2004) (7.1 km s $^{-1}$ after correcting it for a distance of 414 pc to the ONC), and Sánchez et al. (2008) (6.9 ± 1 km s $^{-1}$) is still large enough for this component to be escaping from the Trapezium. Indeed, the escape velocity of the OT system is ~ 6 km s $^{-1}$ according to Allen et al. (1974). The space velocity of component E relative to A (the vector sum of 5.5 ± 1.2 km s $^{-1}$ for the separation velocity, and 6.3 ± 2.0 km s $^{-1}$ for the relative radial velocity, see Table 5) is at least 8.3 ± 2.3 km s $^{-1}$, which is larger than the escape velocity of the OT.
- Although component F also appears to be escaping from the system we were not able to confirm its physical membership to the OT. It is probably a foreground star, physically unrelated to the Trapezium. Using

the photometric data of Da Rio et al. (2009) and Muench et al. (2002) we find that the visual total extinction (A_v) of star F is at least 0.4 mag smaller than that of the bright Trapezium components, adopting the spectral type of component F (B8) given by Herbig (1950). This result places F in front of the OT, probably in the foreground veil (O’Dell et al. 2001), and is consistent with its belonging to the abundant stellar population in front of the Trapezium Cluster proposed by Alves & Bouy (2012).

- The velocity dispersion we find for components A, B, C and D is 1.1 km s^{-1} in one coordinate. Component E is escaping, component F is probably a foreground star, hence, they have not been considered in this estimate. Of course, a velocity dispersion based on only four stars is of doubtful significance, but it is consistent with the OT being a bound system. Even if we include component E, the velocity dispersion in one coordinate increases only to 1.8 km s^{-1} . The value we estimate is comparable to that found by van Altena et al. (1988) (1.37 km s^{-1} , when adjusted to a distance of 414 pc) for a much larger sample of member stars of the ONC. This velocity dispersion is significantly smaller than that found by Jones & Walker (1988) for a larger sample of ONC stars but, as these authors remark, if they restrict their sample to the brighter stars, those with magnitudes comparable to the van Altena et al. (1988) sample, the conflict practically disappears. For these stars, Jones & Walker (1988) obtain a velocity dispersion of 1.31 km s^{-1} (adjusted to a distance of 414 pc). The velocity dispersion we find, although from a very small number of (bright) stars, is comparable to that of van Altena et al. (1988) and to the Jones & Walker (1988) bright sample. The space motions, particularly that of component C, remains a controversial subject. A comprehensive discussion can be found in O’Dell et al. (2009). Briefly, van Altena et al. (1988) find a motion of $4.8 \pm 0.5 \text{ km s}^{-1}$ towards PA 142 degrees, significantly larger than the velocity dispersion of the ONC; Tan (2004) inter-

preted this velocity as evidence that the BN infrared and radio source object (which is moving in the opposite direction) originated in the OT. However, later studies of the radio sources in the embedded BN-KL cluster region (Rodríguez et al. 2005; Gómez et al. 2005) found three radio sources moving away from a common point where they coincided some 500 years ago, and showed that the source used by Tan (2004) as reference was one of the moving objects.

Photographic determination of astrometric positions of stars is notoriously difficult and van Altena’s tangential motion of 4.8 km s^{-1} is almost certainly too high (O’Dell et al. 2009). van Altena et al. (1988) find a poor agreement of their proper motion of component C with that found by McNamara (1976). Indeed the motions obtained by McNamara are, in units of mas yr^{-1} , $\mu_x = -8.3$, $\mu_y = -5.7$, quite incompatible with those found by van Altena et al. (1988), $\mu_x = +1.4 \pm 0.17$, $\mu_y = -1.8 \pm 0.17$. The data from van Altena et al. (1988) indicate that components B and C are moving in opposite directions at about 3.5 mas yr^{-1} , a result incompatible with the relative motions of these stars found by Allen et al. (1974) who over a time interval of over 125 years, find no significant relative change in their separation. The results of the present study imply a separation velocity of component B relative to C of 0.71 mas yr^{-1} ($1.4 \pm 0.9 \text{ km s}^{-1}$ see Figure 5 and Table 4), also incompatible with the van Altena et al. (1988) result.

- The rest of the components of the OT, present small and random velocities that resemble the behavior of a bound and virialized system as found by Allen & Poveda (1974); Allen et al. (1974, 2004).

5. CONCLUSIONS

Diffraction-Astrometry is a novel technique that permits precise measurements of the relative positions of stars on saturated images. In this work we have made use of this technique to measure 44 WFPC2 images of the OT over a time period of 12 years (1995–2007). We found the relative positions of the six brightest components (A to F)

of the OT and were also able to measure their relative displacements over this time period. To supplement the astrometric results from the HST data, we used a compilation of historical data (~ 200 yrs) for the motion of these components from the WDS. We calculated the relative separation velocities of all the OT components with respect to all the other components as well as the relative rate of change of their PAs. However, the rate of change of the historical PA measurements turned out to be unreliable, and that determined from DA only is not sufficiently accurate due to the short time base.

Our results yield the kinematics of the OT with a mean precision of $\sim 1.0 \text{ km s}^{-1}$. Component E is moving with a velocity larger than the escape velocity of the system; thus, we conclude that it is in the process of escaping the OT, as was found by Allen et al. (2004); Costero et al. (2008); Sánchez et al. (2008). The transverse velocity values of the other components (A, B, C and D) are small and random, mimicking the behavior of a bound and virialized system as indicated by Allen & Poveda (1974); Allen et al. (1974, 2004). The fact that one component of the OT is escaping from this system supports the Allen & Poveda (1974) studies of the dynamics of trapezium-type systems, in which they study the evolution of 30 systems and found that, in a time period of a million years, 13 of them, almost 50 %, would eject one or two components.

We are grateful to DGAPA–UNAM for financial support under project PAPIIT number IN109809 and CONACyT grants I–52081 and I–102284. This work is based on observations made with the NASA/ESA Hubble Space Telescope, obtained from the data archive at the Space Telescope Science Institute. STScI is operated by the Association of Universities for Research in Astronomy, Inc. under NASA contract NAS 5-26555. It also has made use of the Washington Double Star Catalog maintained at the U.S. Naval Observatory.

We acknowledge an anonymous referee for his/her numerous suggestions, which greatly improved this work.

We wish to express our special gratitude to C.R. O’Dell for fruitful discussions and encouragement.

REFERENCES

- Allen, C. and Poveda, A. 1974, IAU Symposium, 62, 239
- Allen, C., Poveda, A. and Worley, C. E. 1974, RevMexAA, 1, 101
- Allen, C., Poveda, A. and Hernández-Alcántara, A. 2004, RevMexAA Conf. Ser., 21, 195
- Alves, J. and Bouy, H. 2012, A&A, 547, A97
- Anderson, J. and King, I. R. 1999, PASP, 111, 1095
- Anderson, J. and King, I. R. 2003, PASP, 115, 113
- Argyle, B. 2004, in *Observing and Measuring Visual Double Stars*, London, Springer-Verlag
- Close, L. M., Puglisi, A., Males, J. R., et al. 2012, ApJ., 749, 180
- Costero, R., Allen, C., Echevarría, J., et al. 2008, RevMexAA Conf. Ser., 34, 102
- Da Rio, N., Robberto, M., Soderblom, D. R., et al. 2009, ApJS, 183, 261
- Dolphin, A. E. 2000, PASP, 112, 1397
- Fruchter, A. and Sosey, M. et al. 2009, *The MultiDrizzle Handbook*, version 3.0, (Baltimore, MD: STScI)
- Gilliland, R. L. 1994, ApJ, 435, L63
- Golimowski, D. A., Fastie, W. G., Schroeder, D. J., et al. 1995, ApJL, 452, L125
- Gómez, L., Rodríguez, L. F., Loinard, et al. 2005, ApJ, 635, 1166
- Gonzaga, S., Biretta, J., et al. 2010, in HST WFPC2 Data Handbook, v. 5.0 (Baltimore, MD: STScI)
- Gualandris, A., Portegies Zwart, S. and Eggleton, P. P. 2004, MNRAS, 350, 615
- Herbig, G. H. 1950, ApJ, 111, 15
- Holtzman, J. A., Burrows, C. J., Casertano, S., et al. 1995, PASP, 107, 1065

- Jeffers, H. M., van Denbos, W. H. and Greeby, F. M. 1963, Publications of the Lick Observatory
- Jones, B. F. and Walker, M. F. 1988, *AJ*, 95, 1755
- Kozhurina-Platais, V., Anderson, J. and Koekemoer, A. M. 2003, Instrument Science Report WFPC2 2003-02 (Baltimore, MD: STScI)
- Kozhurina-Platais, V., Goudfrooij, P. and Puzia, T. H. 2007, Instrument Science Report ACS 2007-04 (Baltimore, MD: STScI)
- Kraus, S., Weigelt, G., Balega, Y. Y., et al. 2009, *A&A*, 497, 195
- Lehmann, H., Vitrichenko E. A., Bychkov V., et al. 2010, *A&A*, 514, A34
- Maíz-Apellaníz, J. 2002, HST Calibration Workshop (eds. S. Arribas, A. Koekemoer, and B. Whitmore), 346
- Mason, B. D., Wycoff, G. L., Hartkopf, W. I., et al. 2001, *AJ*, 122, 3466
- McMaster, Biretta, et al. 2008, WFPC2 Instrument Handbook, Version 10.0 (Baltimore, MD: STScI)
- McNamara, B. J., 1976, *AJ*, 81, 375
- Menten, K. M., Reid, M. J., Forbrich, J., et al. 2007, *A&A*, 474, 515
- Muench, A. A., Lada, E. A., Lada, C. J., et al. 2002, *ApJ*, 573, 366
- O'Dell, C. R. 2001, *ARAA*, 39, 99
- O'Dell, C. R., Henney, W. J., Abel, N. P., et al. 2009, *AJ*, 137, 367
- Olivares, J., Sánchez, L. J., Ruelas-Mayorga, A., et al. 2011, *RevMexAA Conf. Ser.*, 40, 282
- Plaskett J. S. and Pearce, J. A. 1931, *Publ. Dom. Astrophys. Obs.*, 5, 1
- Poveda, A., Ruiz, J. and Allen, C. 1967, *Boletín de los Observatorios Tonantzintla y Tacubaya*, 4, 86
- Preibisch, T., Balega, Y., Hofmann, K. H., et al. 1999, *New Astronomy*, 4, 531
- Rodríguez, L. F., Poveda, A., Lizano, S., et al. 2005, *ApJ*, 627, 65
- Ruelas-Mayorga, A., Sánchez, L. J., Olivares, J., et al. 2011, *PASP*, 123, 1290
- Sánchez, L. J., Ruelas-Mayorga, A., Allen, C., et al. 2008, *RevMexAA Conf. Ser.*, 34, 10
- Sánchez, L. J., Ruelas-Mayorga, A., Olivares, J., et al. 2011, *RevMexAA Conf. Ser.*, 40, 308
- Sánchez, L. J., Ruelas-Mayorga, A., Olivares, J., et al. 2013, *RevMexAA Conf. Ser.*, in press
- Stetson, P. B. 1998, *PASP*, 110, 1448
- Stickland, D. J. and Lloyd, C. 2000, *The Observatory*, 120, 141
- Tan, J. C., 2004, *ApJ*, 607, 47
- van Altena, W. F., Lee, J. T., Lee, J. F., et al. 1988, *AJ*, 95, 1744
- Vitrichenko, E. A. 2002a, *Astron. Letters*, 28, 324
- Vitrichenko, E. A. 2002b, *Astron. Letters*, 28, 843
- Vitrichenko, E. A., Bondar, N. I., Bychkova, L., et al. 2012, *Astrophysics*, 55, 199
- Vitrichenko, E. A., Klochkova, V. G. and Plachinda, S. I. 1998, *Astron. Letters*, 24, 296
- Vitrichenko, E. A., and Klochkova, V. G. 2004, *Astrophysics*, Vol. 47, 169
- Weigelt, G., Balega, Y., Preibisch, T., et al. 1999, *A&A*, 347, L15
- Whitmore, B., Heyer, I. and Casertano, S. 1999, *PASP*, 111, 1559